The role of extensively delocalized π-electrons in electrical conductivity, non-linear optical properties and physical properties of polymers

L. R. Dalton, J. Thomson and H. S. Nalwa
Department of Chemistry, 620 Seaver Science Center, University of Southern California, Los Angeles, California 90089-0482, USA
(Received 7 August 1986; accepted 2 October 1986)

Advanced magnetic resonance techniques, including electron nuclear double resonance (ENDOR) and electron spin echo (ESE) spectroscopies, have been employed to investigate π-electron delocalization (both static and dynamic) and charge transfer effects (both intra- and intermolecular) in a variety of polyacetylene and heteroatomic ladder polymers. The consequences of these measurements for electrical conductivity, non-linear optical activity, and physical properties such as solubility are discussed.

(Keywords: electrically conducting polymers; non-linear optical activity; soliton; polaron; π-electron delocalization; ladder polymer; polyacetylene)

INTRODUCTION

For nearly a decade, polymers with delocalized p–π highest occupied molecular orbitals (HOMO) have been of interest due to their novel electrical conductivity properties. When exposed to electron donating or accepting dopants, electrical conductivities increase from the insulator/semiconductor region to the metallic regime. Moreover, at low doping levels, this behaviour can often be attributed to solitonic or polaronic species. Consequently, substantial effort has been expended attempting to define the wavefunction and dynamics of defect species and in developing models relating these properties to electrical conductivity[1-4].

More recently, large third order optical susceptibilities, χ^3, have been observed for *trans*-polyacetylene[5,6] and several heteroaromatic polymers[7,8]. Theoretical calculations suggest that χ^3 should increase as the sixth power of the electron delocalization length[9,10]. It can be argued that charge transfer effects and electron phonon coupling will also likely have a significant effect on non-linear optical (NLO) activity[5,11]. We also note that it is important to ascertain if defect species dominate χ^3 by establishing the quantitative relationship of soliton or polaron concentrations to NLO activity.

Another feature of delocalized π-electron systems is their fundamental insolubility suggesting strong Van der Waals interactions between the π-clouds of the polymer chains. If this is the case, events such as intermolecular charge transfer should affect solubilities.

In this paper we report the use of advanced magnetic resonance techniques to define the 'time-independent' soliton or polaron wavefunctions in high symmetry polymers, to define defect dynamics, and to define certain intra- and intermolecular charge transfer effects. We relate the results of our experimental observations to non-linear optical activity, electrical conductivity, and physical properties.

Polymers of the form $-(A{=}B)-_x$ have been theoretically investigated by Rice and Mele[12] who have demonstrated the conditions for which the existence of solitons or polarons are expected. Clearly, solitonic behaviour is expected for *trans*-polyacetylene. E.p.r. studies on relatively small heteroatomic molecules (phenazine, 1,4,5,8-tetra-aza-anthracene) establish the equality of $\beta_{C\text{-}C}$ and $\beta_{C\text{-}N}$ Hückel parameters, thus suggesting that soliton/polaron species should exist in $-(C{=}N)-_x$ polymers although transport through nitrogen is predicted to be somewhat retarded relative to carbon[13]. Calculations also suggest that soliton delocalization cannot proceed through groups such as –NH[13]. Thus, ladder polymers such as poly[1,6-dihydropyrazino[2,3-g]-quinoxaline-2,3,8-triyl-7(2H)-ylidene-7,8-dimethylidene (PQL) are expected to exhibit the HOMO delocalization profile shown in *Figure 1*.

The –NH group is expected to participate in π-electron delocalization only through intramolecular charge transfer involving the soliton mid-gap state and the lone pair electrons on nitrogen in –NH.

A variety of theoretical methods[1-4,14-17] have been employed to calculate the fundamental form of the time-

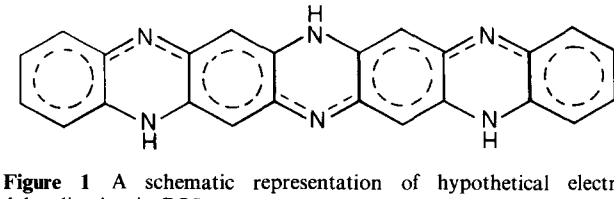

Figure 1 A schematic representation of hypothetical electron delocalization in PQL

0032-3861/87/040543-10$03.00

independent wavefunction of the self-localized soliton defect. It is clear that for polyacetylene a form close to the original SSH[14] prediction is obtained. However, phonons are expected to modulate this intrinsic delocalized wavefunction and in the absence of pinning potentials, phonon modulation would promote translation of the defect along the polymer chain. However, it has been observed that it is impossible to prepare *trans*-polyacetylene by the Shirakawa method[18] without contamination by residual *cis*-polyacetylene[19]. *Cis*-polyacetylene does not have a symmetry appropriate to support soliton defects and thus such segments act to inhibit soliton delocalization in a *cis/trans* polyacetylene copolymer. The ENDOR spectra of *trans/cis* copolymers are observed to depend upon isomer content and upon temperature[20-23]. In *trans*-rich materials near ambient temperature, the proton ENDOR consists of a single line centred at the proton nuclear Larmor frequency and characterized by a peak-to-peak width on the order of 50 kHz[23]. The ENDOR spectrum broadens as the temperature is lowered until a spectrum is obtained at 2 K which is characterized by uniform soliton delocalization over an approximately 70 Å segment (or distribution of segment lengths)[24,25]. For *cis*-rich polyacetylene samples, ENDOR spectra characteristic of a localized soliton are observed even at elevated temperatures although some spectral broadening is observed as the temperatures are lowered[23]. The greatest soliton localization is observed for a *cis*-rich sample of $(^{13}C^{1}H)_x$[26-28]; it may be that $^{13}C/^{12}C$ isotopes act as a symmetry-breaking, localizing perturbation. Although a uniformly delocalized wavefunction is observed in *trans/cis* polyacetylene copolymers and in *trans*-polyacetylene segments in composites with structural polymers[29,30], the self-localized wave function predicted by theory[14] has yet to be observed.

Pulsed microwave (ESE) techniques have been employed to define soliton dynamics[31-34]. The frequency dependence of electron spin–lattice and spin–spin relaxation times has been determined in order to gain insight into the dimensionality of soliton dynamical processes[23]. Electron spin–lattice relaxation for *trans*-polyacetylene samples is dominated by fast, 1-D modulation of electron–electron dipolar interactions. The temperature dependence of electron spin–lattice relaxation rates require electron–phonon interaction with a correlation time on the order of 10^{-13} s at ambient temperatures[34]. While this is the timescale for modulation of the soliton–nuclear interaction and hence the mid-gap levels, the modulation may not produce long range soliton translational diffusion if such diffusion is opposed by pinning or localization potentials. We have unsuccessfully attempted to detect fast, long range soliton diffusion employing electron spin echo magnetic field gradient techniques[35]. This result, together with ENDOR and ESSEEM data indicating short range electron delocalization, suggests that pinning potentials or intrinsic self-localization forces act to confine (on short time scales) the soliton defect to narrow (<100 Å) regions.

Strong evidence does exist for longer range, intermediate (on the order of hyperfine frequencies) frequency dynamics. The observation of a minimum[36-39] in the electron spin echo phase memory time over the same temperature range (from 4–300 K) coupled with the temperature dependence of ENDOR spectra described earlier suggests modulation of hyperfine interactions by dynamical frequencies on the order of 10^6–10^8 Hz. Detailed analysis of ENDOR and ESE data suggests that the dynamics are activated and described by an activation energy on the order of k (200–400 K), where k is the Boltzmann constant.

Studies of transient oxygen exposure indicate that oxygen likely participates in peroxide crossbridges which in turn act to retard soliton diffusion[40]. The apparent activation barrier depends upon the number of such crossbridges.

Because of the many problems encountered with Shirakawa polyacetylene, much recent effort has been focused upon synthesis of polyacetylene by alternative means and upon investigating other polymer systems which are hopefully free from contamination by catalyst, peroxide and carbon–carbon crossbridges, and non-soliton-supporting isomers. Also, it is important that the polymers exhibit at least limited solubility and hopefully liquid crystalline solution behaviour permitting the polymers to be extruded into ordered films and fibres. The polymers should be physically strong and chemically stable. The present work will particularly focus upon efforts to develop such systems.

EXPERIMENTAL

Trans-rich polyacetylene (*t*-PA) samples were prepared by both the Shirakawa[18] and Durham[41-43] synthetic procedures. It will be recalled that the Durham method involves preparation of *t*-PA via a soluble precursor polymer route (see *Figure 2*).

Partially aligned *t*-PA was prepared by mechanically stretching the precursor polymer followed by thermal elimination (*in vacuo*). The dynamics of the soliton defect in Durham polyacetylene samples are dramatically influenced by residual fluoroxylene (1,2-bis(trifluoromethyl)benzene elimination product which is trapped to some extent in the polymer lattice. As will be discussed later, fluorooxylene acts to pin the soliton and to impose a local mode relaxation[44] on the pinned soliton. The detailed kinetics of fluoroxylene elimination and *cis/trans* isomerization has recently been investigated[43].

The ladder polymer PQL was prepared by the following condensation reaction[45] (*Figure 3*) where

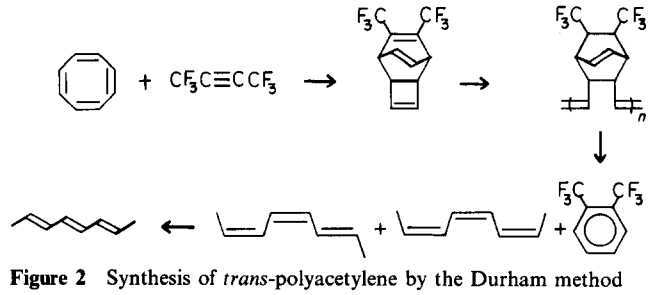

Figure 2 Synthesis of *trans*-polyacetylene by the Durham method

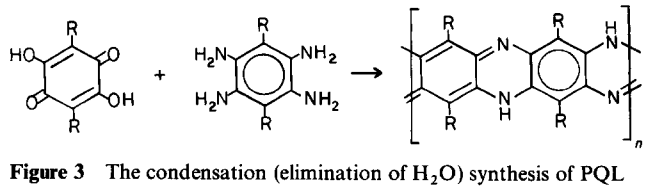

Figure 3 The condensation (elimination of H_2O) synthesis of PQL

R = H, $-C_{11}H_{23}$, or $-OC_{20}H_{41}$. In this communication, we will focus upon results obtained with R = H. The details of the synthesis of ladder polymers by conventional and sequential synthetic methods[46] will be presented elsewhere[47]. For the present, we simply note that particular care was taken to purify monomers used in the various condensation reactions. All material and sample handling was performed in a Vacuum Atmospheres glove box kept under argon atmosphere. The glove box was further equipped with both an oxygen analyser and a moisture analyser; at no time, unless otherwise indicated, were any of the samples exposed to more than 1 ppm of oxygen or 2 ppm water vapour. All of the samples were subsequently sealed in commercial grade or Suprasil quartz e.p.r. tubes under helium atmosphere to insure better thermal contact. Samples of ladder polymers were stored at either 77 K or 250 K while polyacetylene samples were normally stored at 77 K.

POL (poly[2H,11H-bis[1,4]oxazino[3,2-*b*:3′,2′-*m*]triphenodioxazine-3,12-diyl-2,11-diylidene-11,12-bis(methylidine)]) and PTL (poly[2H,11H-bis[1,4]triazino[3,2-*b*:3′,2′-*m*]triphenodithiazine-3,12-diyl-2,11-diylidene-11,12-bis(methylidine)]) were prepared[48] according to *Figure 4* where X = O (POL) or S (PTL).

BBL (poly[(7-oxo-7,10-benz[de]imidazo[4′,5′:5,6]-benzimidazo[2,1-*a*]isoquinoline-3,4:10,11-tetrayl)-10-carbonyl]) and BBB (poly[6,9-dihydro-6,9-dioxobisbenzimidazo[2,1-*b*:1′,2′-*j*]benzo[lmn]phenanthroline-2,13-diyl]) were prepared according to[49-51] *Figure 5*. In all cases, the preferred reaction medium was polyphosphoric acid (PPA).

Samples of PBT (poly-*p*-phenylenebenzobisthiazole) were provided by T. E. Helminiak and W. W. Adams of the Wright-Aeronautical Laboratories.

E.p.r. and ENDOR spectra were recorded employing an IBM/Bruker ER/200D e.p.r. spectrometer equipped with an ER/251 ENDOR accessory and a Varian E-109 Century Series e.p.r. spectrometer equipped with an E-1700 ENDOR accessory. All three commercially available ENDOR cavities (operating in TE or TM modes) were employed. Both spectrometers were equipped with field/frequency lock units for stabilization and with variable temperature accessories for temperature variation and control. Microwave frequency was constantly monitored employing an EIP model 545A frequency counter. An IBM/ Bruker model ER/035M-RS Gaussmeter was used to calibrate magnetic field scans.

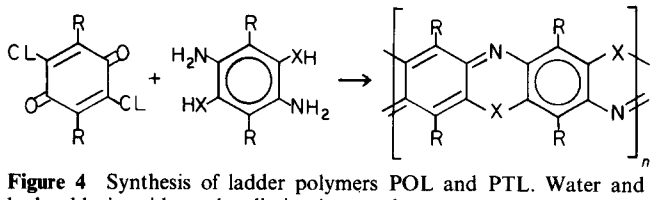

Figure 4 Synthesis of ladder polymers POL and PTL. Water and hydrochloric acid are the elimination products

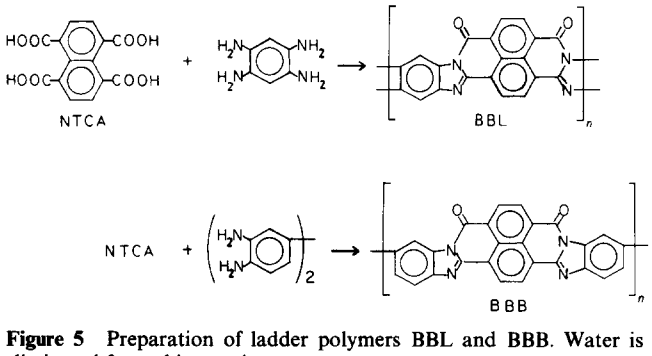

Figure 5 Preparation of ladder polymers BBL and BBB. Water is eliminated from this reaction

Electron Zeeman (*g*-factor) interactions were measured using the EIP counter to determine microwave frequency, ν. Known reference samples (Na^+TCNE^-/THF, $g = 2.002766 \pm 0.000002$[52]; perylene cation in concentrated sulphuric acid, $g = 2.002564 \pm 0.000002$[53]; and PD-tempone (or ^{15}N-PD-tempone) in toluene-d_8, $g = 2.00602 \pm 0.00005$[54]) were used to calibrate the d.c. magnetic field absolutely according to $H_{ref} = h\nu/g\beta$ where h is Planck's constant and β is the Bohr magneton. The field difference between the reference sample resonance and that of the polymer sample was measured employing the Gaussmeter and was checked by utilizing the known isotropic hyperfine coupling constants of the reference samples (Na^+TCNE^-/THF, $a(^{14}N) = 1.56 \pm 0.02$ Gauss; perylene/sulphuric acid, $a(^1H) = 3.53$, 3.08, and 0.46 Gauss; PD-tempone/toluene-d_8, $a(^{14}N) = 14.572$ Gauss). The *g*-value of the polymer sample was then calculated according to $g_{eff} = h\nu/\beta H$. Cross-correlation of data for various reference samples indicated an absolute accuracy of better than ± 0.0001. Some comments about the relationship between measured *g*-factors and the highest occupied molecular orbital of the polymer are appropriate. If an unpaired electron resides in an atomic p orbital, the components of the electron Zeeman tensor are related to the spin–orbit coupling constant, ξ, of the atomic p orbital by[55]

$$g_x = g_y = 2.0023 - (2\xi/\Delta E)[\langle P_0|L_x|P_{+1}\rangle\langle P_{+1}|L_x|P_0\rangle + \langle P_0|L_x|P_{-1}\rangle\langle P_{-1}|L_x|P_0\rangle]$$

$$= 2.0023 - (2\xi/\Delta E)$$

$$g_z = 2.0023$$

$$g = (1/3)(g_x + g_y + g_z) = 2.0023 - (4\xi/3\,\Delta E)$$

where ΔE is the optical gap. Different atoms will have different spin–orbit couplings associated with their valence π-orbitals, e.g. $\xi(C) = 28\,cm^{-1}$, $\xi(N) = 76\,cm^{-1}$, $\xi(O) = 151\,cm^{-1}$, and $\xi(S) = 382\,cm^{-1}$. In a polymer, the paramagnetic electron is not expected to be localized on one atom but rather is anticipated to reside in a delocalized molecular orbital (MO) described as a linear combination of atomic orbitals (LCAO). The observed *g* shifts will depend upon the spin–orbit coupling constants of the individual atomic orbitals and the extent to which each atomic orbital participates in the HOMO. This participation defines the spin density at various nuclei and, as we shall shortly see, can be defined by electron nuclear double resonance spin density measurements. In reality, this picture is somewhat oversimplified but *g*-value shifts can be estimated by molecular orbital methods such as the Energy Weighted Maximum Overlap (EWMO) method[56].

In addition to *g*-value measurements, e.p.r. linewidth and spin concentration measurements were routinely carried out. As discussed elsewhere[39], care was exercised to avoid errors associated with Zeeman overmodulation, modulation frequency sidebands, and microwave saturation effects. For selected polymer samples, e.p.r. measurements were also executed at microwave frequencies of 500 MHz; 1, 3, 22, 35, and 96 GHz as well as at 9.5 GHz. Magnetic susceptibilities were measured at *x*-band employing the aforementioned commercial

spectrometers, at low frequencies (10–100 MHz) employing a homemade Schumacher–Slichter spectrometer, and employing a SHE corporation SQUID susceptometer. Spin concentrations on the order of 10^{18} spins/g are typically observed for the samples discussed in this communication.

ENDOR spectra were taken employing either radiofrequency FM or AM modulation although the former was clearly preferred for disordered polymer samples as the superior baseline stability obtained with FM modulation makes the analysis of hyperfine tensor elements more reliable. The frequency-synthesizer-generated radiofrequency fields were free from harmonic content and care was taken not to overdrive amplifiers. The effect of modulation, microwave field intensity, and radiofrequency amplitude were thoroughly investigated for each sample at all measurement temperatures. ENDOR measurements were made at temperatures as low as 5 K employing an Oxford model CF1204A Continuous Flow Helium Cryostat. Samples discussed in this paper are disordered powders or films but measurements have also been carried out on partially oriented films. The ENDOR of all samples have been investigated over the temperature range 15–300 K, and the results have been compared with the results of a full range of electron spin echo (ESE) experiments[57]. ESE experiments provide detailed insight into time-dependent electron delocalization but we shall note simply that such measurements have been employed in the present case to verify the conclusions reached from ENDOR data. ENDOR transition frequencies can normally be assigned by inspection and hyperfine frequencies, A_i, can be calculated directly from the associated pair of ENDOR transition frequencies, namely, $A_i = \nu_+ - \nu_-$, which derives from the eigenvalue relationship

$$\nu_\pm = [(\nu_p \pm |A_x/2|)^2 \sin^2\theta\cos^2\phi + (\nu_p \pm |A_y/2|)^2 \sin^2\theta\sin^2\phi + (\nu_p \pm |A_z/2|)^2 \cos^2\theta]^{1/2}$$

Assignments were checked by full spectral simulations obtained by solving the full stochastic Liouville-density matrix equation as discussed elsewhere[58,59]. Spin densities are obtained from proton and nitrogen isotropic hyperfine coupling constants (computed as one third the trace of the respective hyperfine tensor) by use of the relationships $\rho_C = a(^1H)/Q_{CH}$ and $\rho_N = a(^{14}N)/Q_N$ where $Q_{CH} \propto Q_N \simeq 26$ Gauss[60].

While the details of quantitative computer simulation of ENDOR spectra of π-electron polymers is beyond the scope of this communication, a few cautionary comments are appropriate. It is noted that 'passage' effects and nuclear spin diffusion effects influence the ENDOR of all of the samples considered here. Because of passage effects, it is important to define 'in-phase' spectra as signal shapes are observed to change dramatically with the phase setting of the phase-sensitive-detector. Nuclear spin diffusion provides an important mechanism for nuclear spin polarization (in addition to the direct common level effect[23]) and is responsible for non-zero ENDOR signal intensity near the nuclear Larmor frequency. A variety of dynamical events influence ENDOR spectra including motion of residual fluoroxylene in the Durham polyacetylene lattice. This particular motion is manifest in a dependence of ENDOR transition linewidths upon transition frequency (hyperfine interaction). Such effects can often be treated within the framework of time-dependent perturbation theory[61]. Electron Heisenberg spin exchange can also influence ENDOR spectra[30,62] and is a particularly bothersome effect as it can prove difficult to separate spin diffusion effects from actually spatial transport of the soliton defect. A few comments about 'orientation selection' in the ENDOR of randomly oriented materials is also necessary. If spectral dispersion in an e.p.r. spectrum arising from electron Zeeman anisotropy is much greater than hyperfine anisotropy and if spectral diffusion mechanisms such as Heisenberg spin exchange do not act to couple spin packets of the e.p.r. spectrum, then the ENDOR spectra will depend upon the portion of the e.p.r. spectrum saturated and monitored; indeed, the ENDOR spectra resemble those obtained for single crystals. At the other extreme where spectral dispersion is dominated by hyperfine interactions or where packets are effectively coupled by spectral diffusion mechanisms[61], 'powder-like' ENDOR spectra are obtained and these do not depend upon the portion of the e.p.r. spectrum saturated and monitored. The latter case is expected to apply for the ENDOR of delocalized π-electron polymers. While at first consideration the ENDOR of a partially oriented film might be expected to yield higher resolution and be more easy to analyse, such is not the case. Indeed, in the case of partial order, one must know *a priori* the precise orientational distribution before ENDOR spectra can be interpreted. For disordered materials, one, of course, always knows the orientational distribution function.

RESULTS AND DISCUSSION

Typical graphs of the temperature dependence of the magnetic susceptibility are given in *Figures 6* and *7*. Clearly, the polymers represented are paramagnetic and the defect concentrations are sufficiently high to suggest that the defects are intrinsic. This conclusion is also supported by the stability of the defect concentration with various polymer processing procedures. The results shown for POL and BBB are typical for the polymers

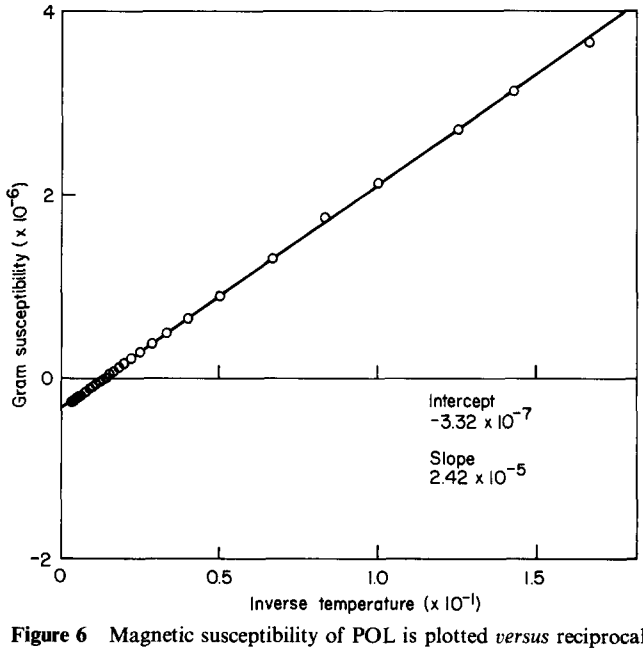

Figure 6 Magnetic susceptibility of POL is plotted *versus* reciprocal temperature

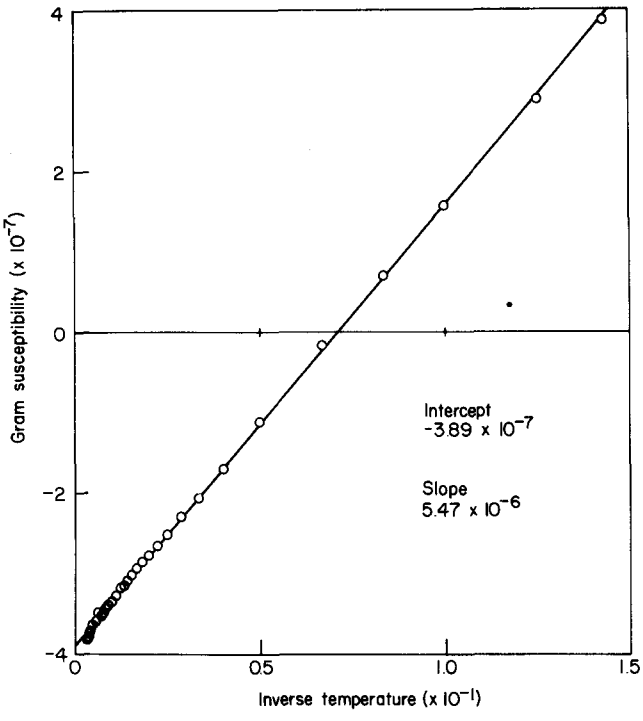

Figure 7 Magnetic susceptibility of BBB is plotted *versus* reciprocal temperature

considered here and spin concentrations are typically of the order of 10^{18} spins/gram.

As the ENDOR spectra of delocalized electron polymers are in general temperature dependent and influenced by noticeable passage effects, a comprehensive discussion of results is not a trivial task. In the following, we concentrate on just a few representative spectra which demonstrate localization effects and one dimensional delocalization phenomena.

In *Figure 8*, we show a typical proton ENDOR spectrum obtained for a polycrystalline sample of BBL at intermediate temperatures (e.g. 250K). The spectrum consists of two components, namely, a strong distant ENDOR signal centred at the proton Larmor frequency with a width typical of nuclear–nuclear dipolar interactions and a local ENDOR spectrum shifted from the proton Larmor frequency by finite, time-independent electron–proton hyperfine interactions. The local ENDOR spectrum exhibits a symmetry clearly suggestive of the anisotropic proton hyperfine interaction arising from a single proton alpha to a p-π orbital on carbon containing finite unpaired electron density. As expected, the ENDOR spectrum is of the powder type and assignments of the turning points of the spectrum to respective elements of the proton hyperfine tensor are indicated in the Figure. Note that the ENDOR spectrum has two branches consistent with the relationship

$$\nu_{\pm} = \nu_p \pm |A_i|/2$$

ENDOR transition probabilities are readily generated by time-dependent perturbation theory as discussed by Dalton and Kwiram[61]. A typical graph or stick diagram of such probabilities (neglecting linewidth effects) is given in *Figure 9*. Such a simulation supports the first order analysis discussed above. More detailed simulations are, of course, required to extract dynamical information from spectra and thus to have a realistic appreciation of the temperature dependence of spectra and of passage effects.

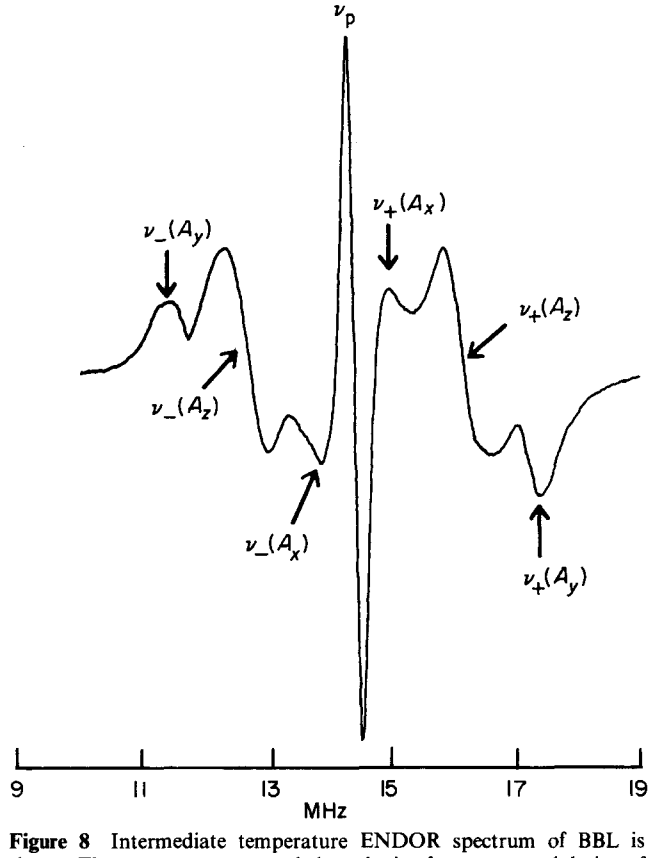

Figure 8 Intermediate temperature ENDOR spectrum of BBL is shown. The spectrum was recorded employing frequency modulation of the radiofrequency field (no field modulation) and first harmonic detection

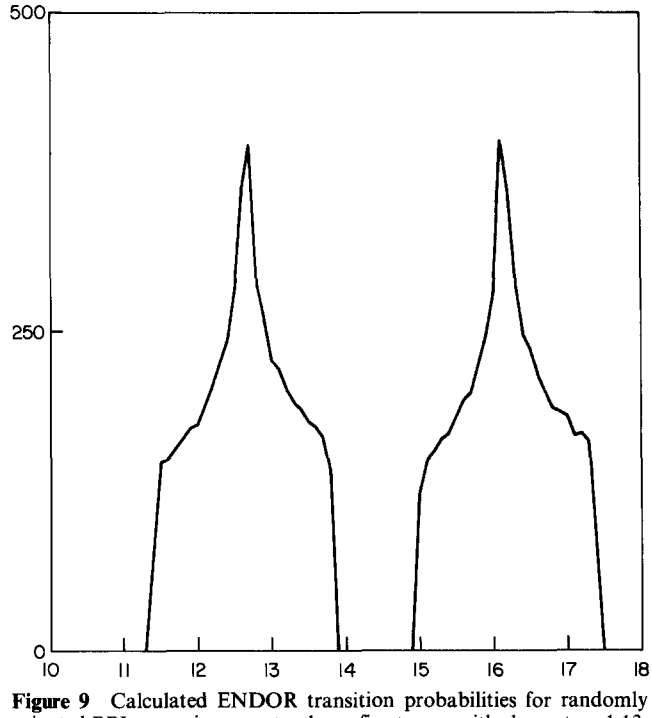

Figure 9 Calculated ENDOR transition probabilities for randomly oriented BBL assuming a proton hyperfine tensor with elements −1.13, −2.52, and −3.48 MHz

The spin density at carbon, ρ_C, is readily extracted from the isotropic component of the proton hyperfine tensor, $a = (1/3)(A_x + A_y + A_z)$, by use of the McConnell relationship $\rho_C = a/Q_{CH}$. The observation of just one proton hyperfine interaction (one unique spin density at carbon) suggests uniform delocalization of the

paramagnetic electron over a 22 atom segment, e.g. where the unpaired electron is assumed to be delocalized over all atoms except nitrogens 7 and 12 shown in *Figure 10*. This uniform delocalization is disrupted when the sample is cooled to lower temperatures as shown in *Figure 11*.

The magnitudes of the hyperfine interactions suggest that the extent of delocalization is not significantly changed. It should, however, be noted that the assignment of spin densities at various carbon positions (at lower temperatures) is not possible at this time and requires ENDOR measurements on samples with selective ^{13}C isotopic enrichment. A ^{14}N ENDOR spectrum is observed centred at approximately 5 MHz. Because of ^{14}N quadrupolar coupling, in addition to nuclear Zeeman and electron nuclear hyperfine interactions, the ^{14}N ENDOR spectrum is complex and analysis of ^{14}N hyperfine interactions is only approximate. To first order, we determine $a(^{14}N) \simeq a(^{1}H)$ and using the relationship $\rho_N = a(^{14}N)/Q_N \simeq a(^{14}N)/26$ Gauss, we conclude $\rho_N \simeq \rho_C$ consistent with uniform electron delocalization.

Similar results are obtained for the other ladder polymers BBB, POL, PTL, and PQL; results for the high symmetry (some 1-D averaging) case are summarized in *Table 1*.

To illustrate arguments supporting uniform electron delocalization for the ladder polymers at intermediate temperatures, it is appropriate to consider the ENDOR of POL, PTL, and PQL further since spin density

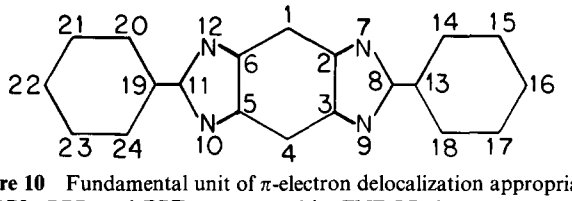

Figure 10 Fundamental unit of π-electron delocalization appropriate for BBL, BBB, and PBT as suggested by ENDOR data

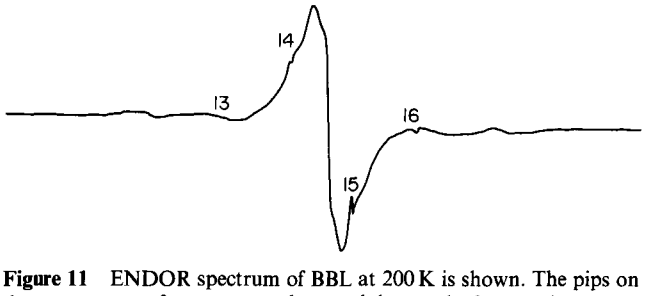

Figure 11 ENDOR spectrum of BBL at 200 K is shown. The pips on the spectrum are frequency markers and denote the frequencies (MHz) indicated

Table 1 Unpaired spin densities at carbon for π-electron polymers and corresponding delocalization lengths

Polymer	$a(^{1}H)$, Gauss	ρ_C	N
Shirakawa	−1.53	+0.06	25 (49)
t-PA	+0.44	−0.02	24
Durham	−2.86	+0.11	15 (29)
t-PA	+0.99	−0.04	14
POL (X=O)	−1.970	+0.076	13–14
PTL (X=S)	−1.945	+0.075	13–14
PQL (X=NH)	−1.713	+0.066	13–14
BBL	−1.236	+0.048	21–23
BBB	−1.156	+0.045	21–23

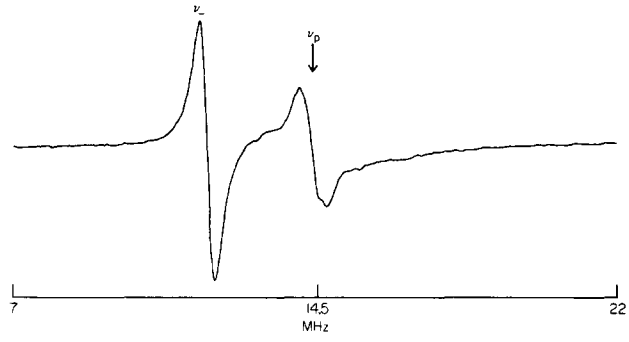

Figure 12 ENDOR spectrum of PQL at 295 K

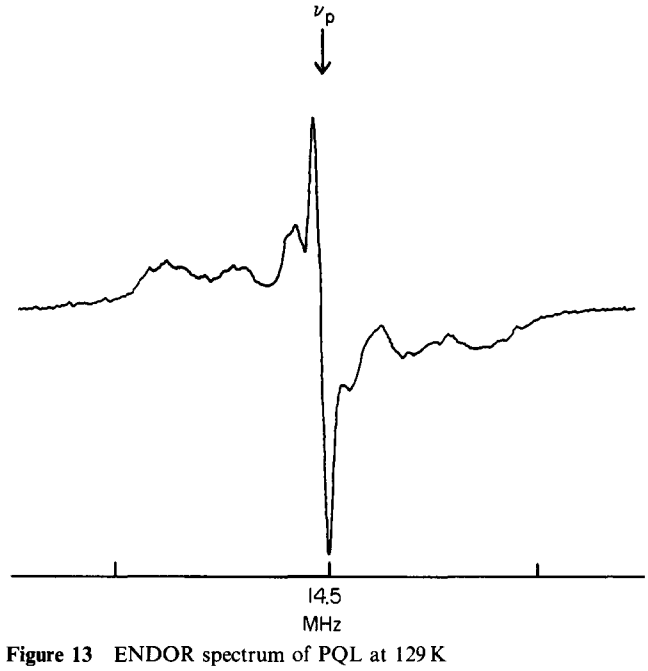

Figure 13 ENDOR spectrum of PQL at 129 K

determinations for these polymers can be compared with those for model compounds such as phenazine[60] and 1,4,5,8-tetra-azanthracene[60]. However, before undertaking this comparison it is appropriate to emphasize the importance of relaxation effects in influencing ENDOR spectra. In *Figure 12*, the ENDOR spectrum for a sample of PQL at 295 K is shown. At this temperature and for the instrumental settings employed, the ν_+ region is apparently missing. However, at other instrumental settings and other temperatures, the ν_+ transitions can be observed. As discussed elsewhere[59,63], spectra such as shown in *Figure 12* are indicative of strong cross (W_x, $W_{x'}$) relaxation effects which arise from modulation of hyperfine interactions. The ENDOR structure observed in the vicinity of ν_p likely arises from hyperfine interaction involving the amine proton (–NH). As with BBL, when the temperature is lowered, the uniform electron delocalization is disrupted and a spectrum is obtained which is suggestive of several hyperfine interactions (see *Figure 13*).

Again, the approximate magnitudes suggest that the extent of delocalization is not significantly different from the high temperature case.

Consider the schematic representation of a ladder polymer segment shown in *Figure 14*. The determination of a single spin density at carbon for the ladder polymers POL, PTL, and PQL requires either that the spin densities at carbon positions 1 and 4 (and by symmetry 5

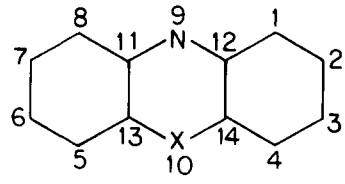

Figure 14 Schematic representation of the ladder polymers POL, PTL, PQL is shown with atomic positions numbered to facilitate comparison of ENDOR results with spin density measurements for 14 atom heteroatomic model compounds. ENDOR data for the polymers suggest that the unit shown represents the fundamental extent of electron delocalization in the polymer materials

and 8) are equal or that the spin density at position 1 is approximately +0.7 while the spin density at carbon 4 is zero. This latter case is unlikely because in odd alternative polyene systems, electron coulomb interactions produce negative spin densities at positions predicted to be nodes in the HOMO wavefunction by Huckel theory. Comparison of our measurements with those for small molecule model compounds such as phenazine provides useful insight into spin density values at various sites including those which are magnetically inactive in our polymer materials[2,3,6,7]. For the phenazine radical anion[60], a proton hyperfine interaction of −1.93 Gauss is observed for carbon 1 (a value very close to the values ranging from −1.713 to −1.970 Gauss observed for this position in the ladder polymers). For phenazine, a value of −1.61 Gauss is observed for position 2. By symmetry, a −1.93 Gauss interaction also obtains for positions 4, 5, and 8 while a −1.61 Gauss interaction obtains for positions 3, 6, and 7. For spin densities at the carbon and nitrogen positions to sum to unity, the value at position 12 (and by symmetry also at 11, 13, and 14) must also be equal to that at positions 1 and 2 suggesting uniform spin densities at all carbon positions. Another example is provided by the radical anion of 1, 4, 5, 8-tetra-aza-anthracene[60]. Uniform spin densities are observed at positions 1, 2, and 9 (by symmetry, also at positions 3, 4, 5, 6, 7, 8, and 10). However, spin conservation (in the case of all positive spin densities) requires spin densities at carbon positions 11, 12, 13, and 14 to be zero. A more serious problem is that of rather poor agreement between spin densities measured for phenazine and 1, 4, 5, 8-tetra-aza-anthracene and spin densities calculated for these radical anions employing molecular orbital theory. For the present, we can only argue that a comparison between the experimental data and data for the model compounds suggests that the fundamental unit for electron delocalization is that shown in *Figure 14* for POL, PTL, and PQL. This can be considered the shortest delocalization extent which is compatible with the experimental data and the assumption of no negative spin densities. The conclusion to be derived from this picture is that NLO activity is not likely to depend upon polymer length. Indeed, macromolecules synthesized from reactions such as that shown in *Figure 15*, may yield the same non-linear optical activity as the PQL polymer. The primary advantage of a polymer would then derived from the physical properties of the polymer including the ability of a polymer to be processed into a variety of forms, thermal stability, mechanical strength, molecular orientation, etc.

Similar arguments hold for the compounds BBL, BBB, and PBT, etc. and the fundamental unit of electron delocalization is the 22 atom unit shown in *Figure 10*.

If we consider the variation of spin densities with X shown in *Table 1*, we note a diminution of spin density at carbon as one progresses from X=O to S to NH consistent with increasing intramolecular charge transfer involving X. Electron Zeeman, g, factors also reflect the participation of X in the HOMO. This conclusion is clear from examination of *Table 2*. Providing valence p-π orbitals are the dominant contribution to g-shifts and given that the contribution to a given orbital is determined by the value for the orbital and by the coefficient of the atomic orbital in the molecular orbital, then we find that the ordering of intramolecular charge transfer as a function of X is NH>S>O consistent with the conclusion derived from the consideration of spin densities. We would, in turn, expect χ^3 values to follow the ordering of intramolecular charge transfer. A particularly attractive possibility is to synthesize polymers which are highly polarized by intramolecular charge transfer. While crystal packing will insure overall electroneutrality, local polarization should insure large NLO effects.

Electrical conductivity for pristine POL, PTL, and PQL appears to follow intramolecular charge transfer but the strong dependence of conductivity upon polymer molecular weight and morphology makes this conclusion rather tenuous.

The delocalized π-electron system has a profound effect upon polymer physical properties including solubility which in turn influences the processing of polymers. Indeed, a major impediment to producing the oriented, thin films necessary for both NLO and electrical conductivity applications derives from the fundamental insolubility. One avenue toward addressing this problem is to take advantage of intermolecular charge transfer between polymer and solvent. Interaction of PBT and BBL with PPA appears to involve adduct formation (see *Figure 16*) and this mode of solvation. We have noted that synthesis of ladder polymers with R other than hydrogen appears to improve the solubility in more conventional solvents such as DMSO. This effect may arise either from steric hindrance involving the R groups which prevents packing of polymer chains to optimize π-electron interactions or may perturb symmetry sufficiently to alter the HOMO distribution.

Detailed ENDOR studies should distinguish between these possibilities. A particularly attractive possibility

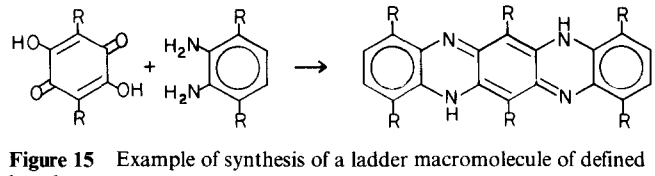

Figure 15 Example of synthesis of a ladder macromolecule of defined length

Table 2 Effective electron g-factors for π-electron polymers

Polymer	g (effective)
t-PA	2.0026
POL	2.00329
PTL	2.00553
PQL	2.00337
BBL	2.0034
BBB	2.0034
PBT	2.0051

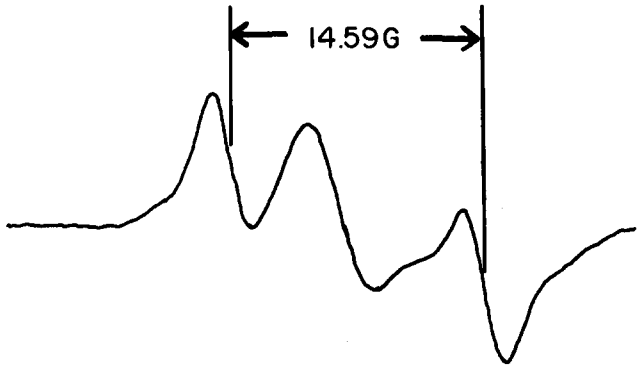

Figure 16 E.p.r. spectrum of PBT showing adduct formation involving PPA (note ^{31}P doublet)

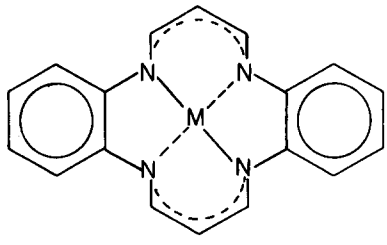

Figure 17 Schematic representation of the metallomacrocyclic unit used in ladder copolymer synthesis

would seem to be the development of R groups to improve solubility and processibility but which could subsequently be eliminated by thermal or photochemical means.

The most desirable centrosymmetric nonlinear optical material is probably one with a large χ^3/α ratio where α is the optical absorption coefficient. A polymer with a small band gap and large α over a substantial range of frequencies may not be particularly useful even if χ^3 is large. In this regard, it is not clear that polymers of solitonic symmetry will yield better materials than those of polaronic symmetry. A factor of importance which has not been addressed to this point is the role of electron–phonon coupling. In addition to the effect on the magnitude of NLO effects, the electron–phonon coupling may well define NLO switching times. Unfortunately, except for *t*-PA, little is known of electron–phonon coupling in delocalized electron polymers.

Because of the relatively short intrinsic electron delocalization lengths in π-electron polymers and because of increasing problems with solubility for longer polymers, we suggest that an important direction in the development of NLO materials would be to investigate shorter chain length polymers prepared by sequential synthesis techniques. Such techniques are also well-suited for the elimination of centrosymmetry necessary for the realization of significant χ^2 values. One of the great advantages of ladder polymers is the synthetic control which can be exercised in producing materials. In addition to the work that we have already demonstrated we note that the *X* position is available for derivatization without directly perturbing the electron delocalization. We also note that we have recently succeeded in preparing copolymers of ladder polymers with the following fundamental metallomacrocyclic unit (see *Figure 17*). When M = Ni we have observed by magnetic resonance measurements a participation of both metal and ligand orbitals in the delocalized HOMO.

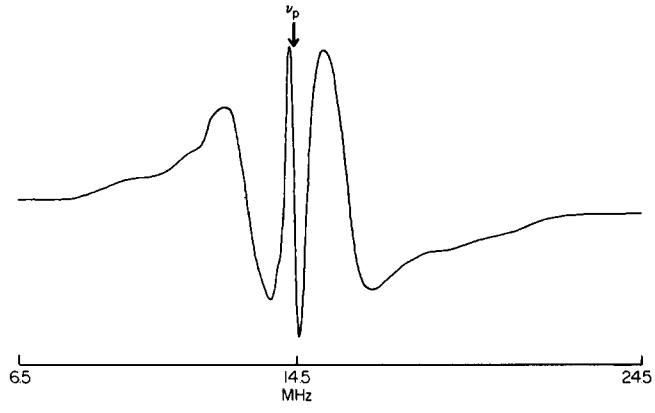

Figure 18 ENDOR of a sample of Durham polyacetylene at 295 K

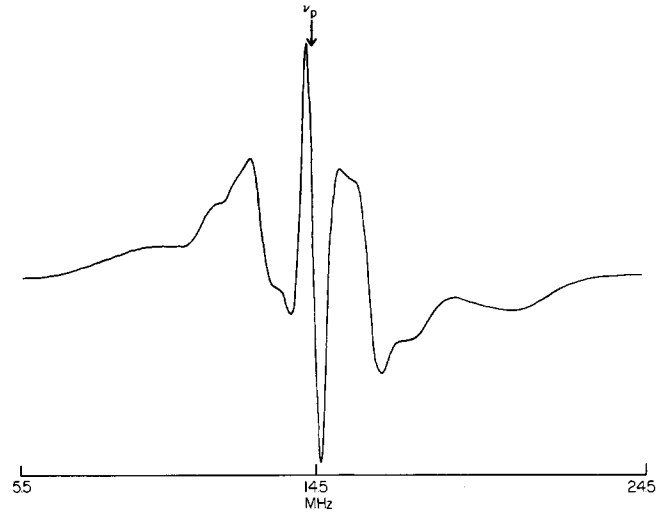

Figure 19 ENDOR of a sample of Durham polyacetylene at 123 K

Typical ENDOR spectra of a Durham polyacetylene samples are shown in *Figures 18* and *19*. The spectrum recorded at a temperature of 123 K is almost identical to that obtained for Shirakawa polyacetylene (the analysis of which has been discussed elsewhere[23,24]). We believe that the best simulation of experimental spectra is obtained employing two spin densities ρ_C(odd carbons) = +0.11 and ρ(even carbons) = −0.04. The simulation of ENDOR transition probabilities is shown in *Figure 20* clearly reproducing the key turning points of the experimental spectrum. Simulations based upon the SSH wavefunction[14] yield spectra devoid of critical turning points[23–25]. Spin densities for Durham and Shirakawa polyacetylene samples are summarized in *Table 1*. Measured spin densities are consistent with an electron delocalization length of approximately 29 carbon units (40 Å).

The temperature dependence of ENDOR spectra of Durham polyacetylene is not unlike that of *cis*-rich Shirakawa polyacetylene; however, electron spin–lattice relaxation behaviour for the two samples is quite different. Electron spin–lattice relaxation in Durham polyacetylene is dominated by a local mode process[44]. The change of ENDOR spectra with temperature suggest modulation of hyperfine interactions probably by the local mode oscillations of fluoroxylene trapped in the polymer lattice. The differences between apparent electron delocalization lengths and relaxation rates for

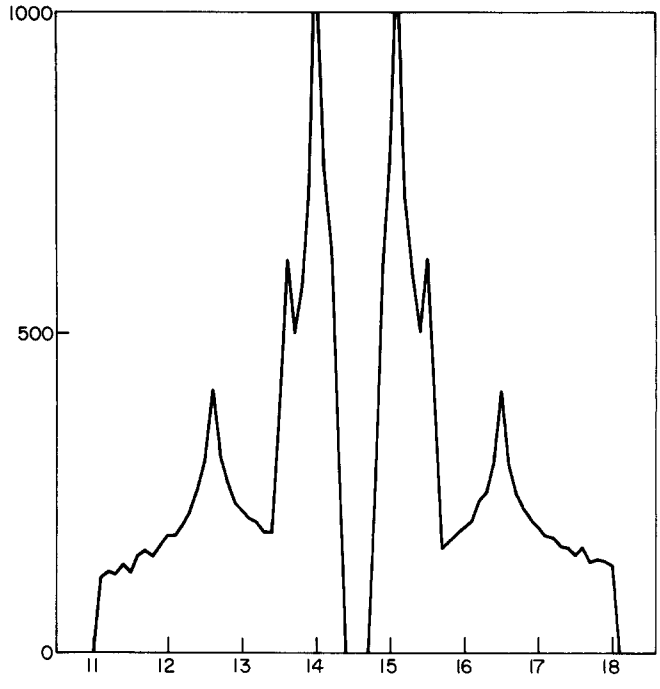

Figure 20 ENDOR transition intensities computed for the proton hyperfine tensors given in ref. 24

different polyacetylene preparations can be associated with lattice effects. Comparison of χ^3 measurements for these materials should elucidate the influence of lattice on nonlinear optical activity.

ACKNOWLEDGEMENT

The research work leading to this paper was performed under Air Force Office of Scientific Research Contract No. F49620085-C-0096 and National Science Foundation Grant No. DMR-8206053.

REFERENCES

1 Etemead, S., Heeger, A. J. and MacDiarmid, A. G. *Ann. Rev. Phys. Chem.* 1982, **33**, 443
2 Epstein, A. J. and Conwell, E. M., Eds. *Proc. Int. Conf. Low Dimensional Conductors, Mol. Cryst. Liq. Cryst.* 1982, **77, 79, 81, 83, 85, 86**
3 Chien, J. C. W. 'Polyacetylene', Academic Press, New York, 1984
4 Skotheim, T., Ed. 'Handbook of Conducting Polymers', Vols. 1 and 2, Dekker, New York, 1985
5 Heeger, A. J., Moses, D. and Sinclair, M. 'Comments on Solid State Physics', to be published
6 Sinclair, M., Moses, D., Heeger, A. J., Vilkelmsson, K., Valik, B. and Salouv, M., private communication to be published
7 Garito, A. F. Work presented at this meeting
8 Prasad, P. N. Work presented at this meeting
9 Rustagi, K. C. and Ducuing, J. *Optics Commun.* 1974, **10**, 258
10 Agrawal, G. P., Cojan, C. and Flytzanis, C. *Phys. Rev. B* 1978, **17**, 776
11 Williams, D. J., Ed. 'Nonlinear Optical Properties of Organic Polymeric Materials', ACS Symp. Ser. 233, Am. Chem. Soc., Washington, D.C., 1983
12 Rice, M. J. and Mele, E. J. *Phys. Rev. Lett.* 1982, **49**, 1455
13 Forner, W., Seel, M. and Ladik, J. *J. Chem. Phys.* 1986, **84**, 5910
14 Su, W. P., Schrieffer, J. R. and Heeger, A. J. *Phys. Rev. Lett.* 1979, **42**, 1698; *Phys. Rev. B* 1980, **22**, 2099
15 Soos, Z. G. and Ramasesha, S. *Phys. Rev. Lett.* 1983, **51**, 2374
16 Boudreaux, D. S., Chance, R. R., Bredas, J. L. and Silbey, R. *J. Phys. Rev. B* 1983, **28**, 6927
17 White, C. T., Kutzler, F. W. and Cook, M. *Phys. Rev. Lett.*, submitted
18 Ito, T., Shirakawa, H. and Ikeda, S. *J. Polym. Sci., Polym. Chem. Edn.* 1974, **12**, 11
19 Gibson, H. W., Weagley, R. J., Mosher, R. A., Kaplan, S., Priest, W. M., Jr. and Epstein, A. *J. Mol. Cryst. Liq. Cryst.* 1985, **117**, 315
20 Thomann, H., Dalton, L. R., Tomkiewicz, Y., Shiren, N. S. and Clarke, T. C. *Mol. Cryst. Liq. Cryst.* 1982, **83**, 33
21 Dalton, L. R., Thomann, H., Tomkiewicz, Y., Shiren, N. S. and Clarke, T. C. *Polym. Prepr.* 1982, **23**, 86
22 Cline, J. F., Thomann, H., Kim, H., Morrobel-Sosa, A., Dalton, L. R. and Hoffman, B. M. *Phys. Rev. B.* 1985, **31**, 1605
23 Young, C. L., Whitney, D., Vistnes, A. I. and Dalton, L. R. *Ann. Rev. Phys. Chem.* 1986, **37**, 459
24 Thomann, H. and Dalton, L. R. in 'Handbook of Conducting Polymers' (Ed. T. A. Skotheim), Vol. 2, Dekker, New York, 1986, 1157
25 Kahol, P. K. and Mehring, M. *J. Phys. C: Solid State Physics* 1986, **19**, 1045
26 Thomann, H., Dalton, L. R., Tomkiewicz, Y., Shiren, N. S. and Clarke, T. C. *Phys. Rev. Lett.* 1983, **50**, 533
27 Dalton, L. R., Thomann, H., Kim, H., Tomkiewicz, Y., Shiren, N. S. and Clarke, T. C. *J. Phys. (France)* 1983, **44**, 229
28 Thomann, H., Dalton, L. R., Grabowski, M. and Clarke, T. C. *Phys. Rev. B* 1985, **31**, 3141
29 Thomann, H., Dalton, L. R., Galvin, M. E., Wnek, G. E. and Tomkiewicz, Y. *J. Phys. (France)* 1983, **44**, 313
30 Dalton, L. R., Thomann, H., Morrobel-Sosa, A., Chiu, C., Galvin, M. E., Wnek, G. E., Tomkiewicz, Y., Shiren, N. S., Robinson, B. H. and Kwiram, A. L. *J. Appl. Phys.* 1983, **54**, 5583
31 Shiren, N. S., Tomkiewicz, Y., Kazyaka, T. G., Taranko, A. R., Thomann, H., Dalton, L. R. and Clarke, T. C. *Solid State Commun.* 1982, **44**, 1157
32 Shiren, N. S., Tomkiewicz, Y., Thomann, H., Dalton, L. R. and Clarke, T. C. *J. Phys. (France)* 1983, **44**, 223
33 Thomann, H., Kim, H., Morrobel-Sosa, A., Chui, C., Dalton, L. R. and Robinson, B. H. *Mol. Cryst. Liq. Cryst.* 1985, **117**, 455
34 Robinson, B. H., Schurr, J. M., Kwiram, A. L., Thomann, H., Kim, H., Morrobel-Sosa, A., Bryson, P. and Dalton, L. R. *J. Phys. Chem.* 1985, **89**, 4994
35 Maresch, G. G., Grupp, A., Mehring, M. V., Schutz, J. U. and Wolf, H. C. *J. Phys. (France)* 1985, **46**, 461
36 Bloom, M., Reeves, L. W. and Wells, E. J. *J. Chem. Phys.* 1965, **24**, 1615
37 Stillman, A. E., Schwartz, L. J. and Freed, J. H. *J. Chem. Phys.* 1980, **73**, 3502
38 Pauls, K. P., MacKay, A. L., Soderman, O., Bloom, M., Tanjea, A. K. and Hodges, R. S. *Eur. Biophys. J.* 1985, **12**, 1
39 Dalton, L. R. 'EPR and Advanced EPR Studies of Biological Systems', CRC Press, Boca Raton, 1985
40 Morrobel-Sosa, A., Thomann, H. and Dalton, L. R. *J. Phys. Chem.*, to be published
41 Edwards, J. H. and Feast, W. J. *Polymer* 1980, **21**, 595
42 Edwards, J. H., Feast, W. J. and Bott, D. C. *Polymer* 1984, **25**, 395
43 Foot, P. J. S., Calvert, P. D., Billingham, N. C., Brown, C. S., Walker, N. S. and James, D. I. *Polymer* 1986, **27**, 448
44 Murphy, J. *Phys. Rev.* 1966, **145**, 241
45 Stille, J. K. and Mainen, E. J. *Macromolecules* 1963, **1**, 36
46 Merrifield, R. B. *J. Am. Chem. Soc.* 1963, **85**, 2149
47 Thomson, J. and Dalton, L. R., to be published
48 Kim, O. K. *Mol. Cryst. Liq. Cryst.* 1984, **105**, 161
49 Van Deusen, R. L. *Polym. Lett.* 1966, **4**, 211
50 Arnold, F. E. and Van Deusen, R. L. *Macromolecules* 1969, **2**, 497
51 Arnold, F. E. and Van Deusen, R. L. *J. Appl. Polym. Sci.* 1971, **15**, 2035
52 Jones, M. T., Kuechler, T. C. and Metz, S. *J. Magn. Reson.* 1973, **10**, 149
53 Segal, B. G., Kaplan, M. and Fraenkel, G. K. *J. Chem. Phys.* 1965, **43**, 4191
54 Dalton, L. R., Robinson, B. H., Dalton, L. A. and Coffey, P. *Adv. Magn. Reson.* 1976, **8**, 149
55 Carrington, A. and McLachlan, A. D. 'Introduction to Magnetic Resonance', Chapman and Hall, New York, 1979, 137
56 Jones, M. T., Thomann, H., Kim, H., Dalton, L. R., Robinson, B. H. and Tomkiewicz, Y. *J. Phys. (France)* 1983, **44**, 455

57 Thomann, H., Dalton, L. R. and Pancake, C. *Rev. Sci. Instrum.* 1984, **55**, 389
58 Dalton, L. A. and Dalton, L. R. in: 'Multiple Electron Resonance Spectroscopy', Freed, J. H. and Dorio, M. M., Eds., Plenum Press, New York, 1979, 169
59 Dalton, L. R. 'Advanced Electron Paramagnetic Resonance Spectroscopy', Wiley, New York, 1987
60 Gerson, F. 'High Resolution ESR Spectroscopy', Wiley, New York, 1970
61 Dalton, L. R. and Kwiram, A. L. *J. Chem. Phys.* 1972, **57**, 1132
62 Thomann, H. and Baker, G. L. *J. Am. Chem. Soc.*, to be published
63 Hochmann, V. L., Zevin, V. Ya. and Shanina, B. D. *Soviet-Physics-Solid State* 1968, **10**, 269